



HAL
open science

Local anisotropy analysis of injection moulded fibre reinforced polymer composites

A. Bernasconi, F. Cosmi, D. Dreossi

► **To cite this version:**

A. Bernasconi, F. Cosmi, D. Dreossi. Local anisotropy analysis of injection moulded fibre reinforced polymer composites. *Composites Science and Technology*, 2009, 68 (12), pp.2574. 10.1016/j.compscitech.2008.05.022 . hal-00509047

HAL Id: hal-00509047

<https://hal.science/hal-00509047>

Submitted on 10 Aug 2010

HAL is a multi-disciplinary open access archive for the deposit and dissemination of scientific research documents, whether they are published or not. The documents may come from teaching and research institutions in France or abroad, or from public or private research centers.

L'archive ouverte pluridisciplinaire **HAL**, est destinée au dépôt et à la diffusion de documents scientifiques de niveau recherche, publiés ou non, émanant des établissements d'enseignement et de recherche français ou étrangers, des laboratoires publics ou privés.

Accepted Manuscript

Local anisotropy analysis of injection moulded fibre reinforced polymer composites

A. Bernasconi, F. Cosmi, D. Dreossi

PII: S0266-3538(08)00209-1
DOI: [10.1016/j.compscitech.2008.05.022](https://doi.org/10.1016/j.compscitech.2008.05.022)
Reference: CSTE 4087

To appear in: *Composites Science and Technology*

Received Date: 12 February 2008
Revised Date: 20 May 2008
Accepted Date: 25 May 2008

Please cite this article as: Bernasconi, A., Cosmi, F., Dreossi, D., Local anisotropy analysis of injection moulded fibre reinforced polymer composites, *Composites Science and Technology* (2008), doi: [10.1016/j.compscitech.2008.05.022](https://doi.org/10.1016/j.compscitech.2008.05.022)

This is a PDF file of an unedited manuscript that has been accepted for publication. As a service to our customers we are providing this early version of the manuscript. The manuscript will undergo copyediting, typesetting, and review of the resulting proof before it is published in its final form. Please note that during the production process errors may be discovered which could affect the content, and all legal disclaimers that apply to the journal pertain.



Local anisotropy analysis of injection moulded fibre reinforced polymer composites

A. Bernasconi¹, F. Cosmi^{2*}, D. Dreossi³

¹ Politecnico di Milano, Dipartimento di Meccanica, Milano, Italy

² Dipartimento di Ingegneria Meccanica, Università degli Studi di Trieste, Trieste, Italy

³ Sincrotrone Trieste, Area Science Park, Basovizza, Trieste, Italy.

Abstract

The fibre orientation distribution in a material sample extracted from an injection moulded plate, displaying the commonly encountered layered shell-core-shell structure, was analyzed. Starting from a micro tomography reconstruction of the sample, instead of trying to isolate each single fibre and measuring its geometrical properties, we derived the components of a fabric tensor from the evaluation of a global anisotropy parameter, the mean intercept length MIL. This parameter, commonly employed for the analysis of biological and geological structures, proved to be an efficient tool for the analysis of the structure of short fibre reinforced composites. The local variations of the degree of anisotropy (ratio of the maximum and minimum eigenvalues of the fabric tensor) from the shell to the core layers of the injection moulded plate could be captured and information about the local average fibre orientation angle was also obtained.

Keywords: E. injection moulding, A. short fibre composites, D. tomography, C. anisotropy

1. Introduction

Composite materials like short fibre reinforced polymers are widely employed for the production of load bearing parts in many industrial sectors. The strengthening effect

* Corresponding author. Tel. +39 040 558 3431, fax +39 040 568 469. *E-mail address:* cosmi@units.it (F. Cosmi)

of fibres is strongly influenced by the relation between fibre length and fibre orientation and the direction of the stresses acting in the component. One of the most commonly employed methods for the production of these parts is injection moulding. By this method, fibre orientation in the component is determined by the dynamics of melt polymer filling the mould cavity and behaving like a viscous fluid. Consequently, fibre orientation results from a complex interaction of two effects:

- shear flow, which tends to align fibres with fluid velocity vectors, usually in proximity of the mould walls and in case of converging streamlines, and
- extensional flow, which arranges the fibres perpendicular to the melt polymer flow, usually observed in case of diverging streamlines and at the flow front under certain conditions (e.g. fountain flow) [1, 2].

These combined effects often lead to formation of a layered structure. In particular, when plates are injected through an edge gate, a skin-shell-core structure is observed. Fibre orientation is almost random in the skin layer (usually very thin), parallel to the melt flow in the shell layer, and perpendicular to the melt flow in the core layer. The effects of this layered structure on the mechanical performances of these materials have been reported [2, 3] and constitute the main difficulty in transferring results of tests performed on standard specimens to real parts.

In fact, in order to use these material safely, it is necessary to measure their impact, tensile and fatigue strength. Tests are usually performed on standard injection moulded specimens, which display a high alignment of fibre along the specimen axis due to the regular geometry enforcing high shear flow. In real parts this effect is less pronounced. Moreover, in components of irregular shape, the fibre orientation pattern is very complex and different fibre orientations may be found through the thickness at the same location. Thus, in order to transfer test results to any real part, it is necessary to correctly evaluate and account for these differences in fibre orientation and length distributions.

Microstructural models for predicting composite strength on the basis of the mechanical properties of constituent materials have been developed, and generally consist of formulae taking into account for both fibre length distribution and fibre orientation distribution [4]. Fibre length distribution in a material sample can be easily determined by separating the fibres from the matrix by burning or hydrolysis and observing them at optical microscope, although further fibre breakage during the extraction cannot be excluded. Measurement of fibre orientations is more difficult, because fibres are dispersed in the matrix and cannot be separated from the matrix without altering their orientation. Consequently, simplifying assumptions on fibre orientation are usually made in order to apply these mechanical models and fibre orientation factors are derived implicitly from tests rather than evaluated on the basis of fibre angles measurement [5].

Moreover, design of parts made of these materials is often supported by analysis tools combining the predictive capabilities of software simulating the injection moulding process and structural analysis software implementing the finite element method. A key factor is the possibility of assigning local stiffness of the elements on the basis of fibre orientation as predicted by the injection moulding simulation software. A continuous function describing the fibre orientation statistically, i.e. the orientation tensor, is often used [6] and its evolution during the injection moulding process is predicted by numerical simulation. In order to assess the validity of these analyses, predicted fibre orientations must be checked against reliable, possibly non destructive, measurements on real parts [7].

Both destructive and non destructive techniques have been proposed for determining fibre orientation over the years. Destructive techniques generally consist of cutting a material sample by a microtome, polishing the surface and analyzing the elliptical footprints left by fibres cut by the sectioning plane by means of image analysis

software. The angle θ between the fibre axis and the direction perpendicular to the cutting plane can be inferred from the eccentricity of the ellipses as $\theta = \cos^{-1}(b/a)$, where a and b represent length of the ellipse semi-axes. A large number of papers describing techniques based on this principle have been published and this method is still used, due to its simplicity and low cost. However, it has been soon highlighted that these measurements are affected by big uncertainties, particularly because of difficulties in deriving volume properties from area-based measurements [8] and in obtaining high angular resolution because of the low eccentricity of the elliptical footprints. Moreover, the same elliptical section may correspond to two symmetrical angles θ and $180^\circ - \theta$ [9]. These limitations can be overcome by special techniques, like successive sectioning [10] and keeping trace of the fibre centres along the sample thickness. Instead of physical sectioning, which requires extreme precision in positioning the slices, confocal scanning laser microscopy has been successfully employed to focus successive sections parallel to each other [9]. Although limited to a maximum depth of 40 μm , as reported in Ref. [11], this optical sectioning method combined with improved image analysis allowed for the reconstruction of the 3D fibre orientation distribution in fibre reinforced polymers with high angular resolution [12].

On the other side, standard non destructive techniques consist of using X-rays to obtain an image projection of the fibres on a plane perpendicular to irradiation direction [13]. Only the fibre orientation of planar distribution of fibres can be thus obtained, and different orientations along the thickness of the sample cannot be captured. In order to obtain a complete spatial distribution description, computed microtomography (μCT) is required. The X-rays produced by the source hit the sample, which is placed on a rotating table and after travelling through structures are collected on the detector plane located downstream. This way a large number of radiographs (projections) of the

sample are taken at small angular increments over a 180/360 degrees rotation. From the projections is then possible to reconstruct the internal 3D microstructure of the sample, using well known mathematical algorithms.

Different methods have been proposed for the analysis of the reconstructed 3D image of the composite internal structure. A first method consists of automatic reconstruction of the fibre distribution pattern [14]. The internal structure of a short glass fibre reinforced polypropylene sample was analyzed in terms of fibre length and orientation distributions by this method. The sample had a fibre content of 13% by volume and it is reported that 60 % of the fibres were missed by this method. A second approach has been described in Ref. [15] in application to a short glass fibre reinforced low density phenolic foam (fibre content 5% by weight, corresponding to 2.7% volume fraction). In this case, the fibres were encased in the foam and thus it was possible to transform each individual reconstructed fibre into a cylindrical body of relatively large dimensions (of approximately 100 μm diameter). By saving the spatial information into stereolithographic file format and using commercial CAD software, the cylinders were then manually selected and length and orientation of each fibre could be computed. Obviously, this kind of approach is only possible for a material with relatively low fibre content and when fibre diameters are sufficiently large with respect to the detector resolution.

Both above mentioned references report analyses conducted using conventional μCT equipment. In this case, images are obtained from the three-dimensional X-ray attenuation coefficient map of the sample, i.e. from its absorption properties. Thus, only materials with large differences in matrix and fibre density can be analyzed. In our work, we used synchrotron light as a source of X-rays. The high spatial coherence of the synchrotron source makes it possible to apply phase contrast radiography techniques that allow the detection of small material inhomogeneities within the specimen,

enhancing the visibility of the fibre borders even in case of fibre characterized by a small diameter and allowing the identification of materials of very similar absorption index, like carbon fibres immersed in a polymer matrix. Moreover, the approach followed for the analysis of the reconstructed volume was different from those reported in the cited references. In fact, instead of deriving the orientation angle of each single fibre, we chose to explore the possibility of capturing the characteristics of the fibre distribution by means of global synthetic parameters, usually applied in geomechanics and biomechanics [16, 17]. Therefore, the local average fibre direction and the degree of anisotropy could be evaluated based on parameters related to the distribution of the different phases in a representative volume, without the need of analyzing and/or reconstructing the geometry of each single fibre.

2. Experimental procedure

2.1 Material

We investigated a sample of short glass fibre reinforced (30% by weight) polyamide 6 (PA6-GF 30), whose fatigue behaviour has already been studied in Ref. [18]. Fibres are made of E glass and have a nominal diameter of 11 μm ; a Gaussian statistical distribution with a mean value of 10.5 μm and standard deviation of 2 μm , was observed by high magnification optical microscopy in a 35% glass fibre reinforced polyamide 6.6 with fibres of the same nominal diameter, produced by the same manufacturer of the material used in this research [19]. Similar results were obtained for another short fibre reinforced polyamide in [20].

The statistical distribution of fibre length is of Weibull type. Average fibre length values depend on injection moulding conditions, shape and thickness of mould cavity and fibre concentration. Typical average fibre length values for PA6-GF 30 range

between 200 and 300 μm , with a maximum value of 1.5 mm, as obtained for a standard ISO 527 specimen of the same material [18], using the method reported in [19].

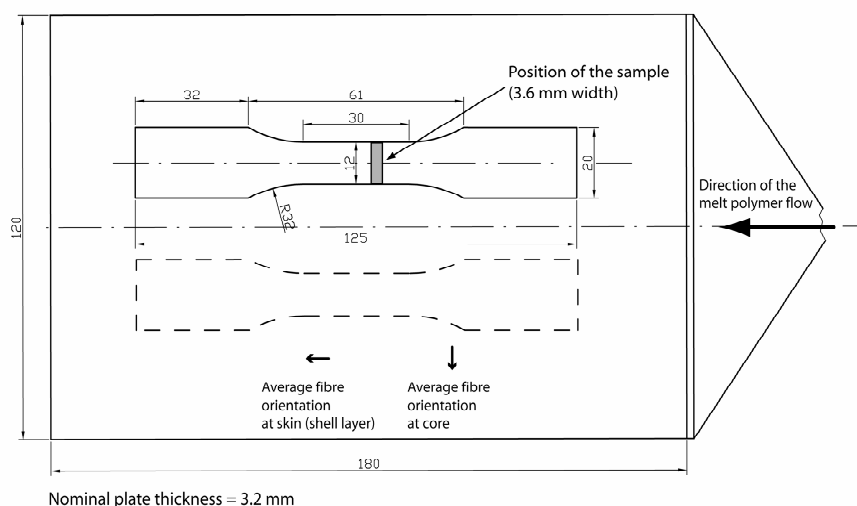


Figure 1 – Specimen used for the extraction of the sample and its position within the injection moulded plate (dimensions in mm).

The specimen examined in this work was extracted from a rectangular plate (nominal dimensions 120 mm x 180 mm x 3.2 mm, actual thickness 3.12 mm), injection moulded through a film gate on the shorter edge. This process ensures a uniform melt polymer flow during the injection process, which enforces a regular mean orientation of fibres in the centre of the plate. In such conditions, fibres in the shell layer are expected to be oriented parallel to the melt polymer flow direction (MPFD), whereas fibres in the core are more likely to be oriented perpendicular to the MPFD. This well defined shell-core structure and the presence in the core layer of fibres oriented perpendicular to the MPFD are visible in Figure 2. This picture was obtained by magnifying at the optical microscope a transverse section of the central part of the specimen, cut perpendicular to its axis. Most fibres display elliptical and small cross-section areas, indicating that they are oriented perpendicular to the section plane. Small portions of fibre, mostly

concentrated in the middle of the picture and corresponding to the core layer of the plate, display long and large cross-section areas, indicating that they are oriented almost parallel to the section plane,.

As described in the following, during micro-CT the sample is rotated and a radiographic projection is taken at each angle. Given the original plate thickness, in order to ensure similar conditions for each projection the sample was cut in the shape of a prism of 3.1 mm x 3.6 mm x 12 mm, as shown in Figure 1. Keeping in mind that spatial resolution and field of view are closely related, details in the order of 10 μ m can also be detected by micro-CT in larger samples (in the order of some centimetres).

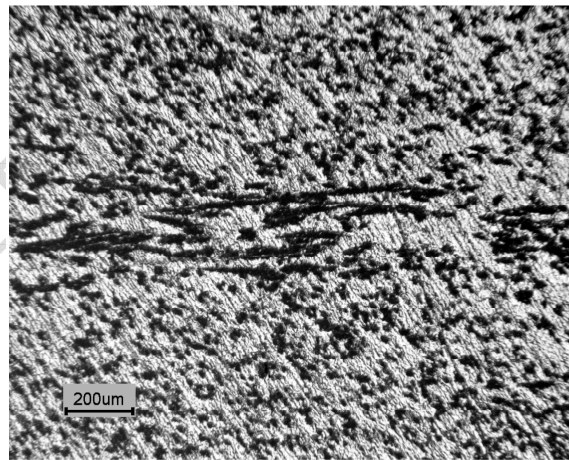
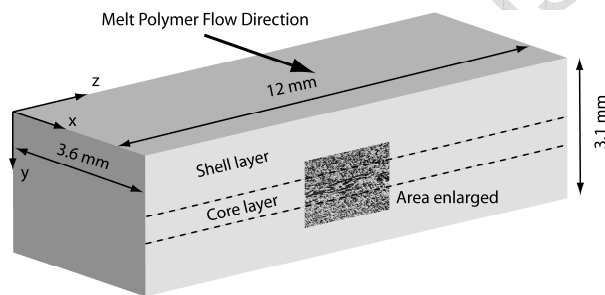


Figure 2 - Polished section perpendicular to the specimen axis: (a) schematic description of the position and (b) optical microscope observation of the observed area within the specimen (fibre in black)

2.2 Data acquisition

The X-ray micro-tomography (μ CT) of the sample using synchrotron radiation was conducted at the SYRMEP beamline of Elettra (Trieste, Italy) [21]. Synchrotron light is an electro magnetic radiation generated by an electron beam bent into a circular trajectory by a system of magnets and, compared to conventional X-ray sources, is characterized by high brilliance and spatial coherence. After the entrance slits systems, the emerging light is made monochromatic by a double-crystal Si (111) monochromator which works in the energy range between 8 keV and 35 keV. The use of monochromatic and laminar-shaped X-ray beams allows, in principle, an improvement of the quality of images. The high spatial coherence of the SYRMEP source makes it possible to apply novel imaging techniques that exploit information of the phase shifts induced by the sample on the radiation field. These phase-contrast techniques [22, 23] are effective to overcome the problems due to poor absorption contrast in the samples, and allow to detect even small inhomogeneities, such as short reinforce fibres inside a polymeric matrix.

At low energies, phase variations are predominant over absorption differences. Thus, by displacing the sensor from the samples in order to detect the phase variations of the rays emerging from the sample, the visibility of constituents with small differences in absorption index is enhanced and images of higher contrast can be obtained. The equipment we used is shown in Figure 3. The detector, made by Photonic Science Ltd, is based on a liquid cooled charge-coupled device camera with to a Gadolinium Oxysulphide scintillator placed on a straight fibre optic coupler, recording images of 4008*2672 pixels of 9 μ m size.

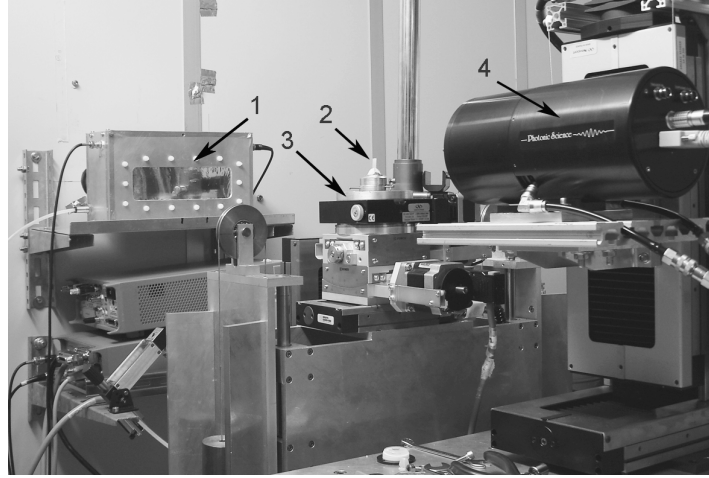


Figure 3 – Microtomography set-up at the SYRMEP beam line: 1. ionization chamber (used to measure the beam intensity); 2. sample; 3. motor driven rotating table; 4. CCD detector

By turning the specimens mounted on a motor driven rotating table at angular steps of 0.25 degrees from 0° to 180°, a total number of 720 projections were recorded by the sensor. Exposure time for each projection depends on sample size, beam parameters and detector characteristics and in our case was of the order of 1 to 2 seconds.

The sample was mounted on the rotating table so that the z axis of the reconstructed volume was aligned with the specimen width direction and the y axis with through-thickness direction (see Figure 2). The x and z axes are the direction within the plane of the plate. The projections were then processed in order to obtain the reconstructed cross-sections (slices) corresponding to each row of pixels in the projection image [24] by using an algorithm based on the filtered back-projection method. Reconstruction of each slice required around 13 seconds with in-house software on a standard PC and a total number of 440 slices were processed. A slice of $3.1 \times 3.6 \text{ mm}^2$ area is shown in Figure 4(a). By stacking the slices along the z direction,

a 3D volume can be reconstructed. A partial reconstruction of a sample volume of $1.8 \times 1.8 \times 1.8 \text{ mm}^3$ is shown in Figure 4(b).

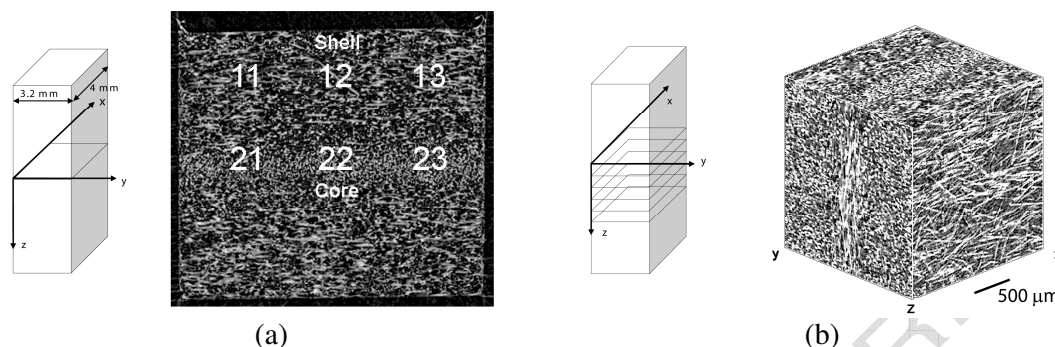


Figure 4 – Reconstructed cross section (2D slice) of the PA6-GF30 sample (a); 3D volume, as obtained by stacking the 2D slices along the z axis (fibre in white).

From this picture, it clearly appears that fibre ($11 \mu\text{m}$ average diameter) is visible in the reconstructed image, despite the relatively low pixel size, $9 \mu\text{m}$. Besides the presence of numerous fibres having a diameter larger than the average one, image contrast at the edges of fibres can also be enhanced by the phase contrast imaging technique adopted in this work.

2.3 Image analysis tools

Instead of trying to reconstruct or to extract information on the geometry of each single fibre, we characterized the anisotropy of our samples by evaluating global parameters. Given the small dimensions and the large number of fibres in our sample, this approach was able to overcome some of the limitations of the methods already described. On the other hand, a global method is bound not to provide a fibre orientation distribution in terms of relative frequencies and orientation angles.

Different definitions of anisotropy exist, depending on the parameter used in the analysis and its relevance for the structure under examination [25]. In this work, we

choose to use the Mean Intercept Length (*MIL*), a parameter commonly used in bio-mechanics [17], which has also been applied to evaluate some characteristics of spatial distributions of reinforcing fibres in polymer composites [26]. For a given structure composed of two different constituents (voids can be considered as a second phase in porous materials), the *MIL* is defined as the average distance between the two phases along a certain direction. To measure the *MIL* of planar distributions, a grid of length L is placed on the image, oriented along a direction indicated by the angle θ as shown in Figure 5. By counting the number $I(\theta)$ of fibre to matrix transitions (matrix to fibre are neglected), the *MIL* is evaluated as

$$MIL(\theta) = \frac{L}{I(\theta)}. \quad (1)$$

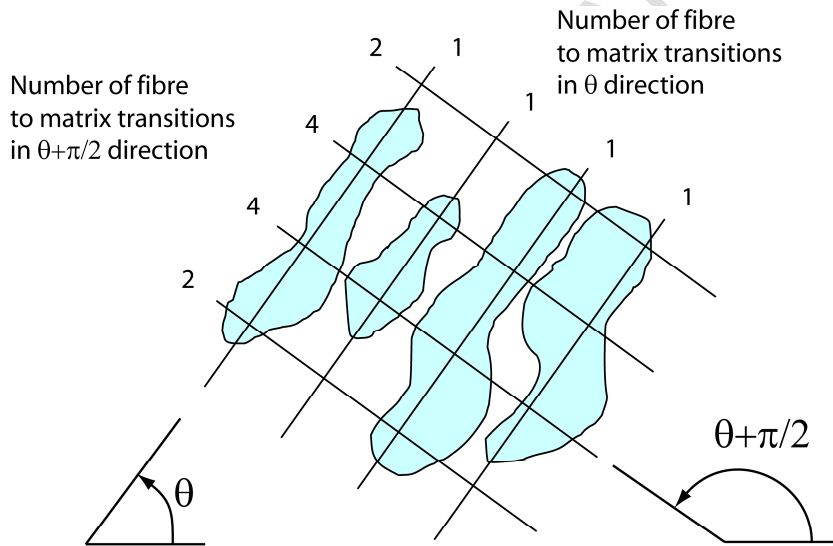


Figure 5 – Example of phase transitions counting for two different rotations at 90° of the grid lines

The *MIL* is a function of the orientation angle θ and higher values are obtained along directions with fewer intersections. In the case of short fibres, these directions are

likely to coincide with the average fibre orientation in case of materials with fibres disposed along a preferred direction. In the case of 3D volumes, the *MIL* must be calculated along different orientations, spanning an entire three dimensional spherical volume. By reporting the *MIL* values in spherical coordinates, in case of structures composed of two phases, the obtained locus of the *MIL* values can be approximated by an ellipsoid and thus transformed into an equivalent second order, positive definite tensor, usually identified as the *MIL* fabric tensor. The eigenvectors of the fabric tensor correspond to the principal directions of the anisotropic structure and the eigenvalues T_1, T_2, T_3 (ordered from the largest to the smallest) are a measure of the distribution of one of the two constituents along the principal directions. For the evaluation of the fabric tensor components we used the software Quant3D [27]. Eigenvalues were normalized by imposing $T_1 + T_2 + T_3 = 1$. The Degree of Anisotropy (*DA*) is also reported, as defined by the ratio $DA = T_1/T_3$.

Size of the Volume Of Interest

A cubic Volume Of Interest (*VOI*) defines the spherical portion used in the analyses, as shown in Figure 6.

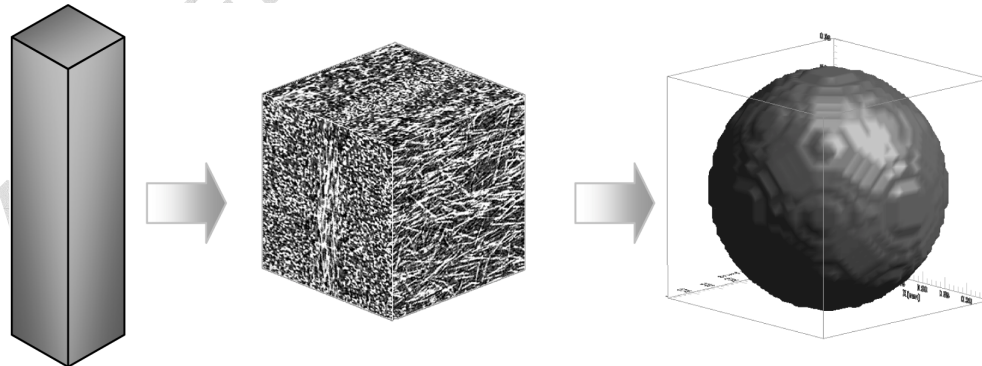


Figure 6 – Example of spherical volume extracted from the reconstructed sample in order to perform *MIL* calculations (fibre in white).

When not differently stated, the results reported in the following sections relate to two portions of $40 \times 40 \times 40$ voxel³, corresponding to a volume of $360 \times 360 \times 360$ μm^3 , extracted from the μCT reconstruction in the shell and the core layer, position 12 and 22 respectively, as shown in Figure 4 (a).

Segmentation

The reconstructed volume is composed of several stacked 8-bit greyscale images, and in order to identify phase transitions, the images require segmentation. Different segmentation methods exist, corresponding to different types of analyses. In our case, a threshold algorithm was used. For simplicity, the threshold was set to the value yielding a Fibre Volume / Total Volume (FV/TV) ratio of 15.7%, corresponding to the volumetric fibre fraction of the composite, as evaluated over the entire reconstructed volume of the micro-tomographed sample of $396 \times 343 \times 413$ voxel³, corresponding to $3.564 \times 3.087 \times 3.879$ mm^3 . In order to allow for comparisons among different volume portions, a unique reference value for the FV/TV ratio, evaluated over the entire available volume, was preferred to the use of a different threshold value for each VOI.

Number of rotations

The results of MIL calculations depend on the number of rotations of the measuring grid at which MIL is computed. The software we used allows for choosing between two values, 513 and 2049 rotations, uniformly distributed over a spherical surface enclosing the VOI as shown in Figure 4. In order to minimize systematic errors, an initial random rotation of the reference grid is performed. The influence of this rotation on the results is shown in Table 1, where the MIL fabric tensor components are reported, as evaluated on a sample extracted from the shell layer with 513 rotations and 1000 measuring lines for each rotation.

Table 1 – Influence of the initial random rotation on the components and principal directions of the *MIL* fabric tensor

	<i>DA</i>		$\cos \alpha$	$\cos \beta$	$\cos \gamma$	
<i>Trial 1</i>	1.82	T_1	0.436245	0.998529	-0.000382	0.054215
		T_2	0.324459	0.00035	0.999038	0.000612
		T_3	0.239296	-0.05422	-0.00059	0.998529
<i>Trial 2</i>	1.82	T_1	0.436202	0.997874	-0.04446	0.047642
		T_2	0.323492	0.046186	0.998295	-0.03569
		T_3	0.240306	-0.04597	0.037811	0.998227
<i>Trial 3</i>	1.80	T_1	0.436052	0.998102	-0.01715	0.059143
		T_2	0.32189	0.018157	0.999698	-0.01656
		T_3	0.242058	-0.05884	0.017604	0.998112

It is clear that the eigenvalues and eigenvectors corresponding to three different initial rotation values are practically coincident. Consequently, in the following, the average of three successive measurements has been always considered. For the same volume samples, the influence of both the number of lines and the number of rotations was evaluated in terms of degree of anisotropy $DA=T_1/T_3$. Results are reported in Table 2 (average of three measurements) and it clearly appears that no significant change in the *DA* values is provided by increasing the number of lines and orientations, whereas the calculation times are raised by a factor of 15. The slight difference in *DA* provided by the combination with the lower values of parameter settings, suggested the adoption of 513 rotations and 1000 lines for the analyses.

Table 2 – Influence of the number of orientations and of the number of lines upon the values of the *DA* and computational time (average of three measurements)

Orientations	<i>Degree of Anisotropy DA</i> (calculation times)		
	500 lines	1000 lines	2000 lines
513	1.82 (t=13s)	1.81 (t=24s)	1.81 (t=48s)
2049	1.81 (t=48s)	1.81 (t=94s)	1.81 (t=188s)

3. Results and discussion

Two volumes of 40^3 voxel were extracted in correspondence of the core and shell layer shown in Figure 4, in positions 12 and 22 respectively. The choice of the dimension depended on the extension of the core layer, in order not to include any portion of the shell layer into the volume representative of the core structure. The software used consents a visual representation of the *MIL* values in each direction in a polar diagram (a so-called rose diagram), which can be compared to the images of the fibre architecture reconstructed by tomography. For example, an image of the fibre layout in the shell layer on a plane parallel to the specimen's longitudinal axis is shown in Figure 7 (a), while the 3D polar plot of the *MIL* values of the same volume is visible in Figure 7 (b). It appears that the maximum value of the *MIL* is found along the x direction, which corresponds to the longitudinal axis of the specimen, indicated by the white arrow in Figure 7 (a). The same type of visual results is reported in Figure 8 (a) and Figure 8 (b) for the sample extracted from the core layer. In this case the maximum value of the *MIL* is found along the z direction, which corresponds to the direction perpendicular to longitudinal axis of the specimen. The values of the principal components T_1 , T_2 and T_3 and the cosine directors of the principal directions of the *MIL* fabric tensor, evaluated as the average over three measures, are shown in Table 3.

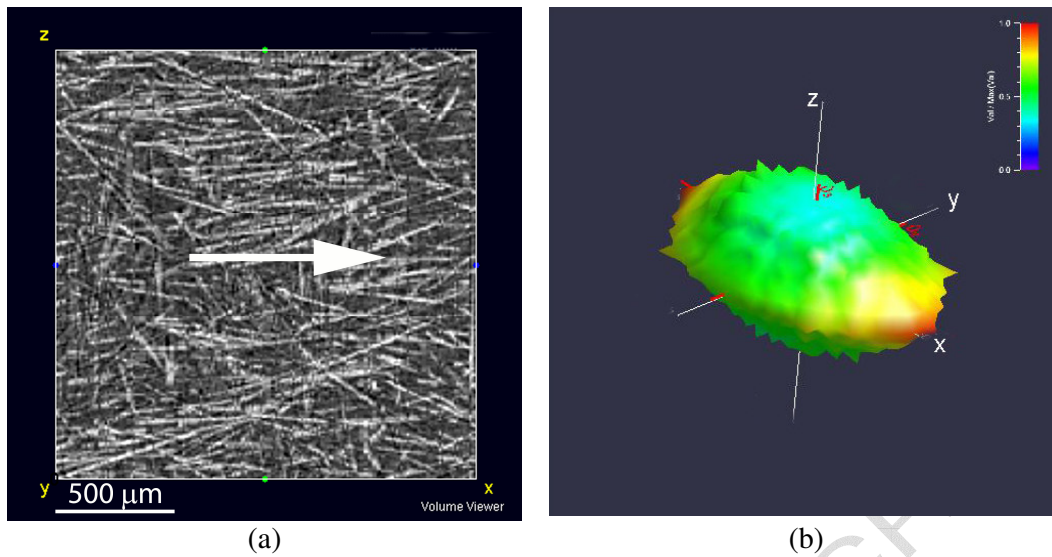


Figure 7 – Tomography reconstruction of the fibre layout in the xz plane of the PA6-GF30 sample extracted from the shell layer; arrow indicates the melt flow direction (fibre in white) (a); three dimensional polar plot of *MIL* values (b)

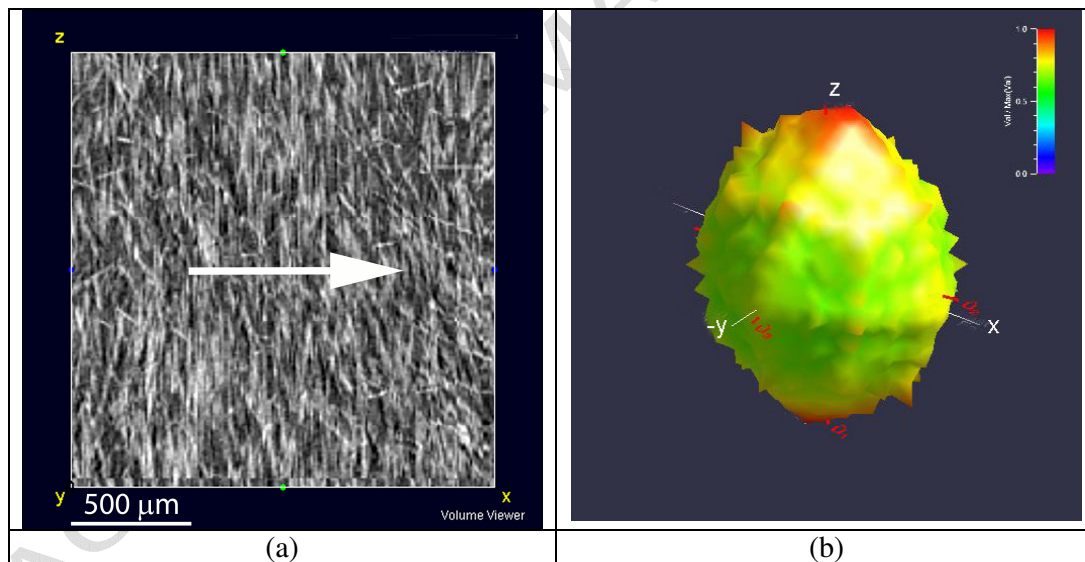


Figure 8 – Tomography reconstruction of the fibre layout in the xz plane of the PA6-GF30 sample extracted from the core layer; arrow indicates the melt flow direction (fibre in white) (a); three dimensional polar plot of *MIL* values (b).

It can be easily verified that the *MIL* fabric tensor parameters are capable of capturing the 90° rotation of the first principal direction, accordingly to the average

fibre orientation that can be deduced from the observation of the pictures of the fibre layout of Figure 7 (a) and Figure 8 (a). Moreover, by comparing the values of the second and third eigenvalues, it can be deduced that in the shell layer a higher degree of fibre alignment along the first principal direction is achieved as compared with the lower values found in the core layer, indicating a higher scatter of fibre orientations.

Table 3– Eigenvalues and cosine directions of the principal directions of the *MIL* fabric tensor of the samples of PA6-GF30 extracted respectively from the shell and core layers of an injection moulded plate. (average of three measurements)

Layer	DA		Eigenvalues	Cosine directors of the principal directions		
				(cos α)	(cos β)	(cos γ)
<i>shell</i>	1.81	T_1	0.4362	0.9982	0.0275	0.0539
		T_2	0.3233	0.0287	0.9993	0.0227
		T_3	0.2406	0.0533	0.0241	0.9983
<i>core</i>	1.22	T_1	0.3667	0.0713	0.1032	0.9921
		T_2	0.3334	0.9816	0.1702	0.0871
		T_3	0.2999	0.1773	0.9800	0.0902

As already stated, the size of the *VOI* in the core layer was dictated by the thickness of the layer itself, which prevented further increase of its size. The greater thickness of the shell layer allowed for a sensitivity analysis of results on the *VOI* size. The analysis was repeated for increasing values of the *VOI*, from $40 \times 40 \times 40$ voxel³ to $120 \times 120 \times 120$ voxel³. The results (average values over three measurements) are reported in Table 4 in terms of degree of anisotropy and first principal direction cosine director $\cos(\alpha)$. By increasing the *VOI* size, the degree of anisotropy increases, the DA values tend to stabilize on a higher value, whereas the first principal direction remains unchanged. The *FV/TV* ratios reported in the table are the values deduced from the analysis of the *VOI* after segmentation, as already explained.

Table 4 – Influence of the VOI size in the shell layer upon the DA and $\cos(a)$ values
(average of three measurements)

<i>VOI</i>	<i>DA</i>	<i>FV/TV</i>	$\cos(a)$ of T_1
40	1.88	0.153	0.9982
80	2.29	0.154	0.9994
120	2.32	0.154	0.9996

By using a relatively small *VOI* size it seems then possible to evaluate the local degree of anisotropy along the thickness of the sample, as well as variations of the principal directions, which can be associated to the mean fibre orientation angle. Results of this type of analysis are reported in Table 5, which refers to six volumes extracted at three different locations in the core and shell layer respectively, as shown in Figure 4. These results verify that the degree of anisotropy is rather uniform in each of the two layers, and confirm the 90 degree shift of the first principal direction in the xz plane between shell and core for all three positions along the x axis. Having assumed the same segmentation threshold for all the volume portions, deviations from the reference value of *FV/TV*, obtained by analyzing different adjacent volumes, can possibly be attributed to local variations of fibre properties such as concentration or diameter, but this could not be verified experimentally.

Our first objective in this research was to test whether the proposed method was able to detect fibre orientation differences between the shell and the core layer. Thus, *VOI* size was required to be large enough in order to provide homogenization within each layer and was principally dictated by the core layer extension. Nevertheless, the same method can be applied even on a smaller scale, provided that *VOI* fibre number and relative dimension are significant.

Although the adopted technique appears to be a promising tool, hopefully allowing for the identification of the local mean fibre orientation, these results should be regarded as initial investigations. The use of the *MIL* fabric tensor to describe the fibre

orientation distribution in short fibre reinforced polymers in terms of mean orientation angle could easily allow for comparison with the same information provided by software simulating the injection moulding process, avoiding the necessity of a complete knowledge of fibre orientation distribution. In fact, the method does not allow for reconstructing the full fibre orientation distribution function, thus preventing the application of some of the available micro-mechanical models based on the fibre orientation distribution, like that of Ref. [4]. On the other hand, we were able to capture the anisotropy properties of samples larger than those that could be analyzed by the other previously published methods, and in considerably lower computation time. In principle, it could be possible to repeat this kind of local analysis in a large number of samples extracted at locations of interest in a real part, thus allowing for an easy comparison of fibre orientations in components with those obtained by means of numerical predictions.

Table 5 – Results (average of three measurements) of the anisotropy analysis of six samples extracted at the locations shown in Figure 4(a)

<i>shell</i>	VOI	11	12	13
	<i>DA</i>	1.80	1.81	2.13
	<i>FV/TV</i>	0.16	0.15	0.20
	T_1	$\cos(\alpha) = 0.9990$	$\cos(\alpha) = 0.9982$	$\cos(\alpha) = 0.9979$
<i>Core</i>	VOI	21	22	23
	<i>DA</i>	1.45	1.21	1.4
	<i>FV/TV</i>	0.23	0.20	0.18
	T_1	$\cos(\gamma) = 0.9926$	$\cos(\gamma) = 0.9921$	$\cos(\gamma) = 0.9858$

The relationship between MIL fabric tensor and fibre orientation tensor, the latter being currently employed to describe fibre orientation in some of the most diffused software packages for injection moulding simulation, has not been established yet. Results published by Bay and Tucker [30], referring to a film gate injection

moulded strip similar to that used in this research, report values of the principal orientation tensor component, related to the degree of fibre alignment along the in flow direction, ranging from 0.9 to 0.8 in the shell layer, and from 0.5 to 0.6 in the core layer. These values are not directly comparable with the *MIL* fabric tensor components reported in Table 3, but some qualitative comparisons are still possible, indicating that these results are consistent with our findings of a lower degree of anisotropy in the core layer ($DA = 1.2 - 1.4$) as compared with the shell layer ($DA = 1.8 - 2.0$), and the 90 degree rotation of the average fibre direction in the plane of the plate.

Finally, further investigation is needed to determine the relationship between the *MIL* fabric tensor and the material properties. In the case of elastic constants, the difficulties consist of relating a second order tensor (the fabric tensor) with a fourth order tensor (the elastic constants). A possible solution could be the assumption of a certain degree of symmetry of the microstructure, enabling to reduce the number of elastic constants to be determined experimentally in order to find the relationships between the components of the two tensors, as for example developed by Cowin [28] and Zysset and Curnier [29] with reference to trabecular bone. Further research will be aimed at verifying the applicability of a similar framework in the case of short fibre reinforced polymers.

Concluding remarks

A method usually applied to the analysis of the microstructure of biological tissues like bones or rock formations has been used to identify the anisotropy properties of a short fibre reinforced polymer. By reconstructing the fibre structure of an injection moulded short glass fibre reinforced polyamide using computed synchrotron micro tomography, 3D images were analyzed in order to evaluate the mean intercept length values for a high number of orientations, covering a spherical volume extracted from

different locations in the sample. On the basis of *MIL* values, the components of the corresponding fabric tensor were evaluated, allowing a local measure of the degree of anisotropy in different portions of the composite. Moreover, by associating the principal directions of the fabric tensor to the mean fibre orientation, results were found to be consistent to the average fibre orientation clearly visible in the layers of injection moulded plates, displaying the often encountered shell/core/shell layered structure.

In this work, we used micro-CT, but in principle *MIL* can be computed from any 3D reconstruction of the volume studied, independently of the technique used to obtain it. Compared to other methods, the evaluation of the *MIL* fabric tensor could not provide the full fibre orientation distribution, however it consented the analysis of samples of relatively larger size in short calculation times. These characteristics could make the proposed technique a powerful tool for the comparison of local fibre structure with results provided by software simulating the injection moulding process.

Acknowledgements

The authors wish to thank ing. Marko Broznic for his contribution to image acquisition and analysis activities. The support by Radici Plastics, Italy, in providing the specimens used in this research, is gratefully acknowledged.

References

- [1] Hull D, Clyne TW. An introduction to Composite Materials. Second Ed. Cambridge Solid State Science Series 1996
- [2] Horst JJ. Influence of fibre orientation on fatigue of short glassfibre reinforced Polyamide. PhD Thesis. TU Delft (Netherland) 1997

- [3] Karger-Kocsis J, Friedrich K. Skin-core morphology and humidity effects on the fatigue crack propagation of PA-6.6. *Plastics and Rubber Processing and Applications* 12 (1989) 63-68
- [4] Fu S, Lauke B. Effects of fiber length and fiber orientation distributions on the tensile strength of short-fiber-reinforced polymers. *Composites Science and Technology* 56 (1996) 1179-1190
- [5] Thomason JL. Micromechanical parameters from macromechanical measurements on glass reinforced polyamide 6,6. *Composites Science and Technology* 61 (2001): 2007-2016
- [6] Advani SG, Tucker CLIII, The use of tensors to describe and predict fiber orientation in short fiber composites, *J. Rheology* 31 (1987) 751-784
- [7] Gupta M, Wang KK. Fiber orientation and mechanical properties of short-fiber-reinforced injection-molded composites: simulated and experimental results. *Polymer Composites* 14 (1993) 367-382
- [8] Bay RS, Tucker III CL. Stereological measurement and error estimates for three-dimensional fiber orientation. *Polymer Engineering and Science* 32 (1992) 240-253
- [9] Clarke A, Davidson N, Archenhold G. Measurements of fibre direction in reinforced polymer composites. *Jornal of Microscopy* 171 (1993) 69-79
- [10] Zak G, Park CB, Benhabib B. Estimation of three-dimensional fibre-orientation distribution in short-fibre composites by a two section method. *Journal of Composite Materials* 35 (2001) 316-339
- [11] Clarke AR, Archenhold G, Davidson NC. A novel technique for determining the 3D spatial distribution of glass fibres in polymer composites. *Composites Science and Technology* 55 (1995) 75-91

- [12] Eberhardt C, Clarke A. Fibre-orientation measurements in short-glass-fibre composites. Part I: automated, high-angular-resolution measurement by confocal microscopy. *Composite Science and Technology* 61 (2001) 1389-1400
- [13] Kim EG, Park JK, Jo SH. A study on fiber orientation during the injection molding of fiber-reinforced polymeric composites (Comparison between image processing results and numerical simulation). *Journal of Materials Processing Technology* 111 (2001) 225-232
- [14] Eberhardt CN, Clarke AR. Automated reconstruction of curvilinear fibres from 3D datasets acquired by X-ray microtomography. *Journal of Microscopy* 206 (2002) 41-53
- [15] Shen H, Nutt S, Hull D. Direct observation and measurement of fiber architecture in short fiber-polymer composite foam through micro-CT imaging. *Composites Science and Technology* 64 (2004) 2113-2120
- [16] Ketcham RA. Three-dimensional grain fabric measurements using high-resolution X-ray computed tomography. *Journal of Structural Geology* 27 (2005) 1217-1228
- [17] Cowin S.C., Doty S.B., *Tissue Mechanics*, Springer, 2007
- [18] A. Bernasconi, P. Davoli, A. Basile, A. Filippi. Effect of fibre orientation on the fatigue behaviour of a short glass fibre reinforced polyamide-6. *Int J Fatigue*.29 (2007) 199-208
- [19] Bernasconi A, Davoli P, Rossin D, Armani C. Effect of reprocessing on the fatigue strength of a fiberglass reinforced polyamide. *Composites Part A*. 38 (2007) 710-718
- [20] Thomason JL. The influence of fibre properties on the performance of glass-fibre-reinforced polyamide 6,6. *Composites Science and Technology* 59 (1999) 2315-2328

- [21] Abrami A et al. Medical applications of synchrotron radiation at the SYRMEP beamline of ELETTRA, Nuclear Instruments and Methods in Physics Research Section A: Accelerators, Spectrometers, Detectors and Associated Equipment, 548 (2005), 221-227
- [22] Snigirev A., et al.: On the possibilities of X-ray phase contrast microimaging by coherent high-energy synchrotron radiation, Review of Scientific Instruments. 66 (1995) 5486-5492
- [23] Fitzgerald R.: Phase-sensitive X-Ray Imaging, Physics Today, 53 (2000), 23-26
- [24] Kak AC, Slaney M(1988): Principles of Computerized Tomographic Imaging, IEEE Press.
- [25] Odgaard A., Three-Dimensional methods for quantification of cancellous bone architecture, Bone 4 (1997) 315-328
- [26] Luo GM , Sadegh AM, Cowin SC, The mean intercept length polygons for systems of planar nets, Journal of Materials Science, 26(1991), 2389-2396
- [27] Ketcham RA, Ryan TM. Quantification and visualization of anisotropy in trabecular bone. Journal of Microscopy 213 (2004) 158-171
- [28] Cowin SC, The relationship between the elasticity tensor and the fabric tensor, Mechanics of Materials, 4 (1985)137-147
- [29] Zysset PK, Curnier A, An alternative model for anisotropic elasticity based on fabric tensors, Mechanics of Materials, 21 (1995) 243-250
- [30] Bay RS, Tucker CL III. Fiber orientation in simple injection moldings. Part II: experimental results. Polymer Composites 13 (1992) 332-341